Preprints of the 21st IFAC World Congress (Virtual)
Berlin, Germany, July 12-17, 2020

Smith predictor embedded analytical fractional-order controller design: A delayed Bode's ideal transfer function approach

Shaival H. Nagarsheth*. Shambhu N. Sharma.**

Sardar Vallabhbhai National Institute of Technology (SVNIT), Surat, Gujarat 395007, India
**(Tel: +91-9727161696; e-mail: shn411@gmail.com, shaival_nagarsheth@ifac-mail.org).*
***(e-mail:snsvolterra@gmail.com)*

Abstract: The main contribution of this paper is to design an enhanced fractional-order controller for the higher-order system. The analytical design methodology utilizes a delayed Bode's ideal transfer function in place of the conventional one as the reference model. A reduced fractional-order plus dead-time transfer function is used to represent a higher-order process. The design also embeds a Smith predictor for the enhanced closed-loop performance. Analytical tuning for the designed fractional-order controller is provided based on frequency domain specifications. The proposed methodology is applied to two higher-order systems, which can be represented by a reduced fractional-order plus dead-time transfer function. The closed-loop performance of the designed controller is compared with that of the three other related controllers. Frequency domain characteristics, load disturbance, sensitivity analysis, and model mismatch performance are demonstrated and compared with those of other controllers as well. The results of the paper reveal that the proposed controller leads to an overall enhanced closed-loop performance.

Keywords: Reduced-order models, delayed Bode's ideal transfer function, fractional-order controller, Smith predictor, sensitivity analysis, robust control.

1. INTRODUCTION

Industrial processes are often represented by higher-order models in order to capture in-depth dynamical behaviour with high accuracy (Isaksson and Graebe, 1999). Many control strategies are available for higher-order processes. They pose a significant challenge to tune the controllers. Isaksson and Graebe (1999) proposed an analytical tuning of integer-order PID for higher-order processes.

Fractional-order controllers have proven superior performance in contrast to integer-order controllers (Podlubny, 1999). Moreover, fractional-order representation of higher-order systems offers a more significant description of the dynamics instead of the integer-order representation (Tavakoli-Kakhki and Haeri, 2011). Fractional-order representation has found places in various forms: fractional-order controllers for fractional-order systems (Malek et al., 2013; Luo et al., 2010), fractional-order controllers for integer-order systems (Monje et al., 2010), and integer-order control for fractional-order systems (Meneses et al., 2019). An Internal Model Control (IMC) based fractional-filter cascaded with integer-order PID was presented by Maâmar and Rachid (2014). They used the concept of Bode's ideal transfer function as the reference model. Moreover, Smith predictor based approach for the design of enhanced fractional-order as well as the integer-order controller has proved their usefulness in recent years (Bettayeb et al., 2017; Araujo and Santos, 2019; Pashaei and Bagheri, 2019). Tuning of the fractional-order controllers is a critical process, failing which, will lead to an unsatisfactory performance (Das et al., 2011). Yumuk et al. (2019) proposed a novel fractional-order controller design for higher-order processes using frequency domain specifications. They considered a reduced-order model known as Non-integer Orders Plus Time Delay (NIOPTD) models (Das et al., 2011).

This paper incorporates a design of an enhanced fractional-order controller using an accurate NIOPTD-I transfer function for the higher-order processes. First, the higher-order processes are approximated by fractional structure, i.e. NIOPTD-I, instead of the integer-order approximation. Second, the Smith predictor (dead-time compensator) is embedded into the inner loop. Then, the proposed controller is designed, where the delayed Bode's ideal loop transfer function is placed in the forward path as a unity feedback reference model. The Bode's ideal transfer function is modified with a delay term in order to account for the time delay of the NIOPTD-I transfer function. Analytical tuning is provided based on the given frequency domain specifications. Stability analysis and numerical simulations of the proposed method are demonstrated for two appealing higher-order processes. Closed-loop performance, frequency-domain characteristics, robustness as well as sensitivity analysis of the proposed method are compared with the methodologies of Bettayeb and Mansouri (2014), Das et al., (2011) and Yumuk et al., (2019). The controller performance indices and the sensitivity performance indices display the enhanced performance of the proposed fractional-filter-fractional-PI controller in this paper.

2. DELAYED BODE'S IDEAL TRANSFER FUNCTION

Bode suggested an ideal transfer function popularly known as the Bode's ideal transfer function (Barbosa et al., 2004)

$$L(s)=\frac{1}{\tau_c s^{\lambda}},\lambda\in\Re, \tag{1}$$

where the gain cross-over frequency $\omega_{gc}=\tau_c^{-1/\lambda}$, i.e., $\left|L(\omega_{gc})\right|=1$. More details are available with Barbosa et al. (2004). Consider unity feedback where Bode's ideal transfer function is placed in the forward path. Then the desired closed-loop transfer function is obtained as

$$CL_{ref}(s)=\frac{1}{\tau_c s^{\lambda}+1}. \tag{2}$$

The closed-loop transfer function (2) is used as a reference model for tuning the controllers. Suppose the desired gain cross-over frequency (ω_{gc}) and the Phase Margin (PM) are given, then fractionality λ and the time constant τ_c are

$$\lambda=\frac{\pi-PM}{\pi/2}-1 \text{ and } \tau_c=\omega_{gc}^{-\lambda}. \tag{3}$$

Now, consider a delayed version of the Bode's ideal transfer function (Yumuk et al., 2019), i.e.

$$L'(s)=\frac{1}{\tau_c s^{\lambda}}e^{-\theta s},\lambda\in\Re. \tag{4}$$

Due to the change in the original form of Bode's ideal transfer function, the new closed-loop transfer function of the unity feedback is given by

$$L_{ref}(s)=\frac{e^{-\theta s}}{\tau_c s^{\lambda}+e^{-\theta s}}. \tag{5}$$

The fractionality λ and the time constant τ_c for (5) are given by

$$\lambda=\frac{\pi-PM-\omega_{gc}\theta}{\pi/2} \text{ and } \tau_c=\omega_{gc}^{-\lambda}. \tag{6}$$

It can be observed from (3) and (6) that the time delay term and the gain cross-over frequency have their contribution in deciding the fractionality, which was not present in the delay less transfer function.

3. CONTROLLER DESIGN

Consider a classical feedback closed-loop structure, as shown in Fig. 1. The feedback consists of a Smith predictor (dead-time compensator) $D_c(s)$ embedded in the inner feedback with controller transfer function $G_c(s)$ in the forward path. The dead-time compensator is defined as $D_c(s)=(1-e^{-\theta s})G^*(s)$, where $G^*(s)$ is the plant transfer function void of dead-time. The unity feedback with the delayed Bode's ideal transfer function in the forward path is shown in Fig. 2.

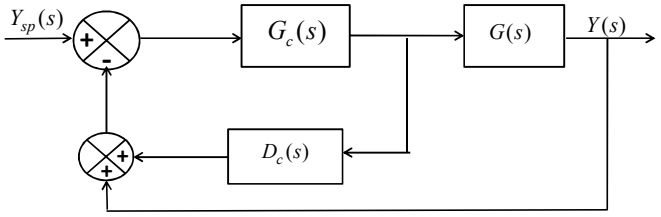

Fig. 1. Classical feedback with embedded Smith predictor.

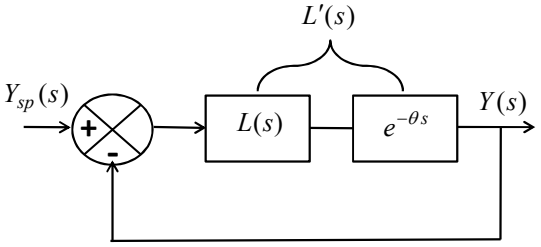

Fig. 2. Reference control-loop with delayed Bode's ideal transfer function.

Using the notion of equivalent systems, the controller transfer function is derived as

$$\frac{G_c(s)G(s)}{1-G_c(s)(G^*(s)-G(s))}=L'(s). \tag{8}$$

Making $G_c(s)$ the subject of formula in (8),

$$G_c(s)=\frac{L'(s)}{G(s)}(1-G_c(s)(G^*(s)-G(s))), \tag{9a}$$

$$G_c(s)=\frac{L'(s)}{G(s)(1+\frac{L'(s)}{G(s)}(G^*(s)-G(s))}. \tag{9b}$$

Equation (9b) is recast as

$$G_c(s)=\frac{L'(s)}{G(s)(1+L'(s)(e^{\theta s}-1))}. \tag{10}$$

Now, One Non-integer Order Plus Time Delay (NIOPTD-I) reduced-order representation of the higher-order processes is given by (Das et al., 2011)

$$G(s)=\frac{K_f e^{-\theta s}}{\tau_f s^{\alpha}+1}. \tag{11}$$

Hence, on substituting the reduced fractional-order transfer function (11) and the delayed Bode's ideal transfer function (4) into (10), we get the fractional-filter-fractional-PI controller, i.e.

$$G_c(s)=\frac{e^{-\theta s}/\tau_c s^{\lambda}}{\frac{K_f e^{-\theta s}}{\tau_f s^{\alpha}+1}(1+\frac{e^{-\theta s}}{\tau_c s^{\lambda}}(e^{\theta s}-1))}.$$

On further simplifications,

$$G_c(s) = \frac{\tau_f s^{\alpha} + 1}{K_f(\tau_c s^{\lambda} + 1 - e^{-\theta s})}. \quad (12)$$

Approximating the delay term with Taylor series expansion in (12)

$$G_c(s) = \frac{\tau_f s^{\alpha} + 1}{K_f(\tau_c s^{\lambda} + \theta s)}, \; G_c(s) = \frac{\tau_f s^{\alpha} + 1}{K_f s^{\lambda}(\tau_c + \theta s^{1-\lambda})},$$

$$G_c(s) = \frac{s^{\alpha-\lambda}}{(\tau_c + \theta s^{1-\lambda})} \frac{\tau_f}{K_f}\left(1 + \frac{1}{\tau_f s^{\alpha}}\right). \quad (13)$$

4. NUMERICAL SIMULATIONS

In this section, the closed-loop performance resulting from the proposed controller (13) is compared with the other three controllers. The comparison is made based: Integral of Square Error (ISE), Integral of Time Absolute Error (ITAE), Integral of Squared Control Input (ISCI), Overshoot (OS), Settling-time (ST), and maximum absolute sensitivity ($S_{\max}$). The fractional-filters are implemented using Oustaloup approximation (Nagarsheth and Sharma, 2020), with $N = 4$, $\psi_h = 10^4$ and $\psi_l = 10^{-4}$.

Example 1

Consider a higher-order system (Yumuk et al., 2019), i.e.

$$H(s) = \frac{1}{(s+1)^3}. \quad (14)$$

NIOPTD-I model for (14) is expressed as (Das et al., 2011)

$$G(s) = \frac{0.9939e^{-1.0006s}}{(2.3298s^{1.0648} + 1)}. \quad (15)$$

The given frequency domain specifications for the closed-loop system are $PM = 80$ and $\omega_{gc} = 0.3 rad/s$. By substituting these specifications in (6), $\lambda = 0.92$ and $\tau_c = 3.0275$ are obtained. Now, utilizing (13), the proposed controller for example 1 is obtained as

$$G_{c(proposed)}(s) = \frac{s^{0.1448}}{(3.0275 + 1.0006s^{0.08})}\left(2.344 + \frac{0.4292}{s^{1.0648}}\right). \quad (16)$$

For the same set of values, the controllers obtained using the methods of Bettayeb and Mansouri (2014), Das et al. (2011), and Yumuk et al. (2019) are as follows:

$$G_c(s) = \frac{2.34267s^{0.0648}}{(1 + 3.80817s^{0.111})}\left(1 + \frac{0.4292}{s^{1.0648}}\right), \quad (17)$$

$$G_c(s) = \left(0.9116 + \frac{0.2526}{s^{1.1577}} + 0.2023s^{0.9973}\right) \quad (18)$$

and

$$G_c(s) = 0.774315s^{0.144789}\left(1 + \frac{0.4292}{s^{1.0648}}\right). \quad (19)$$

Filter fractionality and fractional-PI controller introduces fractionality in the closed-loop characteristic polynomial. The fractional characteristic polynomial can be converted to natural degree characteristic polynomial to assess the stability (Kaczorek, 2011). Then, all the roots of the associated natural degree characteristic polynomial must satisfy the condition $|\angle r_i| > (\delta\pi/2)$, in order to have the proposed closed-loop system stable. Here, r_i denotes the roots of the polynomial and δ is the greatest common divisor. The intricacy of finding the roots of the fractional characteristics polynomial is circumvented by demonstrating the stability analysis graphically via the FOMCON toolbox of MATLAB© (Monje et al., 2010).

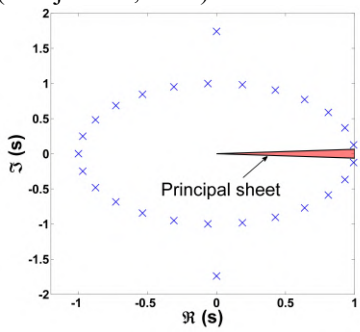

Fig. 3. Stability assessment of proposed controller for example 1

Fig. 3 shows that $|\angle r_i| > (\delta\pi/2)$ holds, as the roots of the associated natural degree characteristic polynomial do not lie inside the principal sheet of the Riemann surface constructed by $(\delta\pi/2)$, where $\delta = 0.04$ for example 1. Thus, the proposed closed-loop system is stable.

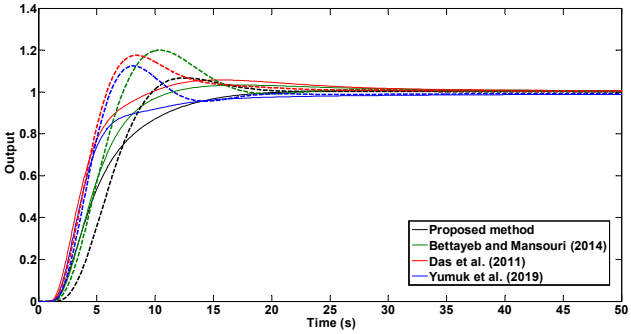

Fig. 4. Closed-loop responses: nominal case, mismatch case associated with example 1.

Figs. 4 and 5 show the closed-loop and load disturbance responses for nominal as well as mismatch cases, respectively. Solid lines denote the nominal case, and the dashed lines denote the mismatch case. The time-domain characteristics with controller performance indices for the nominal case are depicted in Table 1. It can be observed from

Fig. 4 that the proposed controller exhibits 0% overshoot with the least settling time.

Moreover, the ISCI index displays the efforts by the controller, which is least in the case of the proposed method. For the robustness analysis, a 40% mismatch in the plant transfer function (14) parameters is considered. The closed-loop results of reference tracking and disturbance rejection for the mismatch case are displayed in Figs. 4 and 5. In contrast to the other controllers, the proposed controller offers less OS, less ST, and improved performance indices.

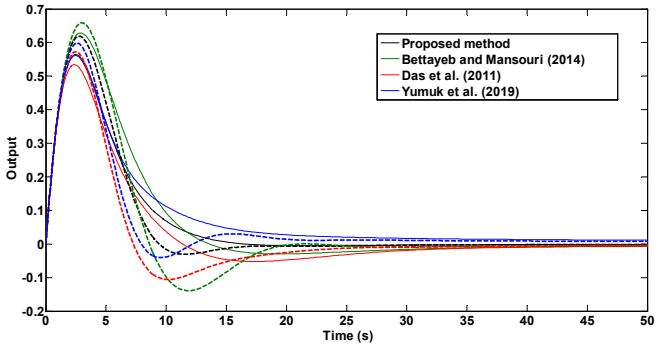

Fig. 5. Load disturbance responses: nominal case, mismatch case associated with example 1.

Table 1. Controller performance indices for the nominal case

Controllers	ISE	ITAE	ISCI	OS (%)	ST
Proposed method	2.01	25.9	45.8	-	16.4
Bettayeb and Mansuri (2014)	2.7	30.18	46.7	3.3	26
Das et al. (2011)	1.9	31.0	61.1	6	28.3
Yumuk et al. (2019)	2.2	32.6	46.6	-	24

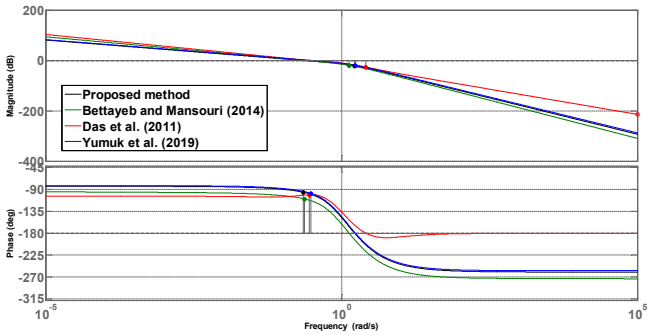

Fig. 6. Comparison of Bode diagrams for example 1.

Bode diagrams for the open-loop transfer function using all the controllers (16)-(19) are shown in Fig. 6. Complimentary sensitivity functions associated with the closed-loop of all the controllers in comparison are displayed in Fig. 7. Fig. 8 shows the absolute sensitivity plots. The inverse of maximum absolute sensitivity $S_{\max}$ denotes the stability margin. Lesser the $S_{\max}$ higher is the stability margin (Åström and Murray, 2008).

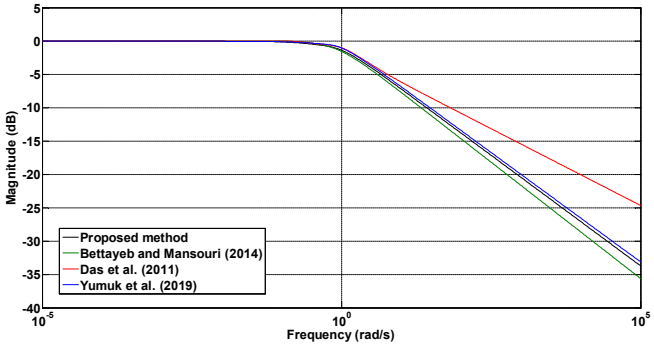

Fig. 7. Complimentary sensitivity graphs for example 1.

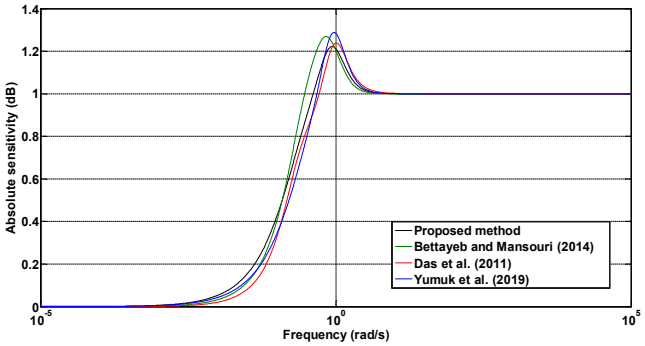

Fig. 8. Graphical illustration of absolute sensitivity for example 1.

From Fig. 7, it can be observed that the controller in Bettayeb and Mansouri (2014) filters the high-frequency signals better in comparison to all the controllers. On the other hand, the proposed control method filters better than the control methodologies in Das et al. (2011) and Yumuk et al. (2019). Moreover, the proposed controller has the least $S_{\max}$ in contrast to all the other controllers (Table 2), which is indicative of better robustness and less amplification occurring due to model mismatch and input disturbances (Fig. 8). Importantly, less $S_{\max}$ resulting from the proposed controller indicates more stability margin in comparison to other controllers.

Table 2. Frequency domain characteristics and sensitivity performance indices for the nominal case of example 1

Controllers	PM	ω_{gc}	$S_{\max}$	ω_{ms}
Proposed method	83.95	0.27	1.22	0.86
Bettayeb and Mansuri (2014)	70.27	0.235	1.27	0.67
Das et al. (2011)	78.66	0.28	1.24	1.01
Yumuk et al. (2019)	81.59	0.3	1.29	0.94

Example 2

Consider a third-order system (Yumuk et al., 2019), i.e.

$$H(s)=\frac{9}{(s+1)(s^2+2s+9)}. \quad (20)$$

NIOPTD-I model for (20) is expressed as (Das et al., 2011)

$$G(s)=\frac{1.0003e^{-0.4274s}}{(0.8864s^{1.0212}+1)}. \quad (21)$$

The given frequency domain specifications for the closed-loop system are $PM=80$ and $\omega_{gc}=1 rad/s$. Thus, we get $\lambda=1.0336$ and $\tau_c=1$. Now, utilizing (13), the proposed controller for example 2 is obtained as

$$G_{c(proposed)}(s)=\frac{s^{0.0212}}{(0.4274+s^{0.0336})}\left(0.88613+\frac{0.9997}{s^{1.0212}}\right). \quad (22)$$

For the same set of values, the controllers obtained using the methods of Bettayeb and Mansouri (2014), Das et al. (2011), and Yumuk et al. (2019) are as follows:

$$G_c(s)=\frac{2.07331s^{0.0212}}{(1+2.3397s^{0.111})}\left(1+\frac{1.1281}{s^{1.0212}}\right), \quad (23)$$

$$G_c(s)=\left(0.8944+\frac{1.2309}{s^{1.0019}}+0.2713s^{0.9355}\right), \quad (24)$$

and

$$G_c(s)=\frac{0.88613}{s^{0.01243}}\left(1+\frac{1.1281}{s^{1.0212}}\right), \quad (25)$$

respectively. Fig. 9 displays the stability assessment of the proposed closed-loop of example 2 on the Riemann surface.

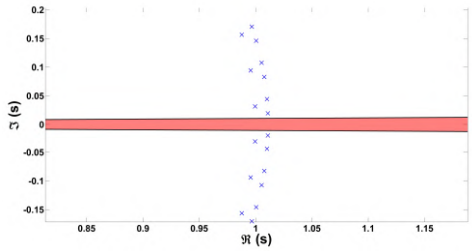

Fig. 9. Stability assessment of the proposed controller for example 2.

Figs. 10 and 11 show the closed-loop and load disturbance responses for nominal as well as mismatch cases, respectively. The time-domain characteristics with controller performance indices for the nominal case are depicted in Table 3. It is evident from Fig. 10 that all the other controllers (23)-(25) possess OS under a 40% mismatch in the gain of the plant. On the other hand, the proposed controller still does not possess OS and is able to provide promising performance without overshoot under model mismatch case. This improvement in the robust performance is due to the contribution of the dead-time compensator in the proposed controller.

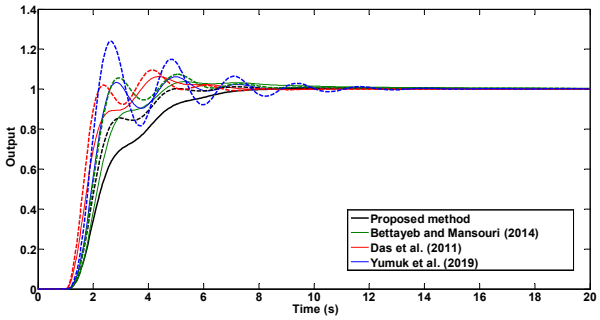

Fig. 10 Closed-loop responses: nominal case, mismatch case associated with example 2.

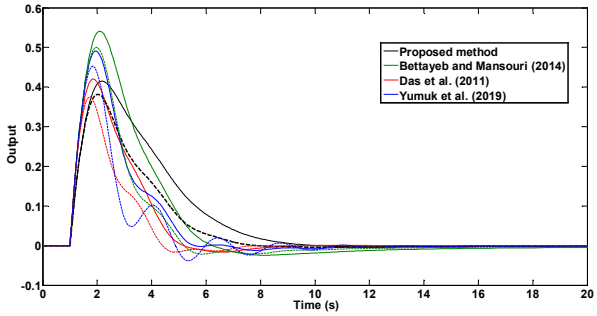

Fig. 11 Load disturbance responses: nominal case, mismatch case associated with example 2.

Table 3. Controller performance indices for the nominal case

Controllers	ISE	ITAE	ISCI	OS (%)	ST
Proposed method	**0.47**	**4.8**	**18.1**	**-**	**6.6**
Bettayeb and Mansuri (2014)	**0.92**	**9.9**	**19.3**	**4.7**	**8.6**
Das et al. (2011)	**0.6**	**7.1**	**28.7**	**6.3**	**6.5**
Yumuk et al. (2019)	**0.75**	**5.0**	**19.7**	**6.1**	**7.5**

Bode diagrams for the open-loop transfer function using all the controllers (22)-(25) are shown in Fig. 12. Complimentary sensitivity functions associated with the closed-loop of all the controllers in comparison are displayed in Fig. 13. Fig. 14 shows the absolute sensitivity plots. The PM in Table 4 clearly shows that the proposed controller achieved the closest PM to the reference model in contrast to the other controllers.

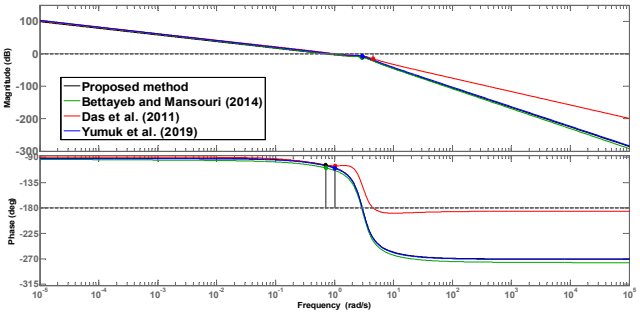

Fig. 12. Bode diagrams comparison for example 2.

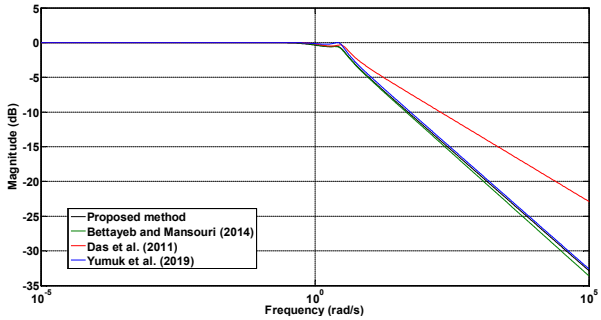

Fig. 13. Complimentary sensitivity graphs for example 2.

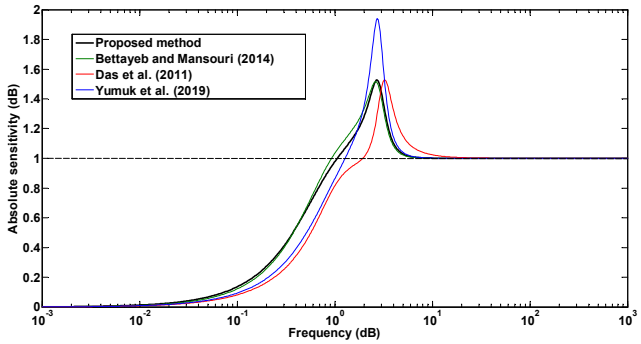

Fig. 14. Graphical illustration of absolute sensitivity for example 2.

Table 4. Frequency domain characteristics and sensitivity performance indices for the nominal case of example 2.

Controllers	PM	ω_{gc}	$S_{\max}$	ω_{ms}
Proposed method	75.7	0.7	1.51	2.725
Bettayeb and Mansuri (2014)	70.7	0.71	1.51	2.603
Das et al. (2011)	74.5	1.02	1.53	3.203
Yumuk et al. (2019)	70.1	1.01	1.94	2.725

6. CONCLUSION

This paper has proposed a fractional-filter fractional-PI controller for higher-order processes, which are represented by the NIOPTD-I fractional-order model. The utilization of the delayed version of the Bode's ideal transfer function instead of the conventional one, as in the other controllers, has lead to the enhanced closed-loop performance of the proposed controller in the sense of improved controller and sensitivity performance indices. The resulting enhanced performance in nominal as well as mismatch case is attributed to the use of the combined effect of Smith predictor and the delayed Bode's ideal transfer function in the controller design. The proposed method also meets the desired frequency domain specifications satisfactorily. It is evident from the comparison of the proposed controller with all other controllers that the controller resulting from the proposed method either achieves the same level or a much better closed-loop performance.

ACKNOWLEDGEMENT

The authors are grateful to the IFAC foundation for considering this work eligible for the Young Author Support (YAS) award. Funding provided to the student author in the form of the YAS award is gratefully acknowledged.

REFERENCES

Araujo, J.M., and Santos, T.L.M. (2019). Control of second-order asymmetric systems with time delay: Smith predictor approach. *Mechanical Systems and Signal Processing*, (in press), 106355.

Åström, K.J., and Murray, R.M. (2008). *Feedback Systems: An Introduction for Scientists and Engineers*. Princeton University Press, New Jersey.

Barbosa, R.S., Machado, J.a.T., and Ferreira, I.M. (2004). Tuning of PID controllers based on Bode's ideal transfer function. *Nonlinear Dynamics*, 38(1-4), 305–321.

Bettayeb, M., and Mansouri, R. (2014). Fractional IMC-PID-filter controllers design for non integer order systems. *Journal of Process Control*, 24(4), 261–271.

Bettayeb, M., Mansouri, R., Al-Saggaf, U., and Mehedi, I.M. (2017). Smith Predictor based fractional-order-filter PID controllers design for long time delay systems. *Asian Journal of Control*, 19(2), 587–598.

Das, S., Saha, S., Das, S., and Gupta, A. (2011). On the selection of tuning methodology of FOPID controllers for the control of higher order processes. *ISA Transactions*, 50(3), 376–388.

Isaksson, A.J., and Graebe, S.F. (1999). Analytical PID parameter expressions for higher order systems. *Automatica*, 35(6),1121–30.

Kaczorek, T. (2011). Selected problems of fractional systems theory, In Thoma, M., Allgöwer, F., and Morari, M. (ed.), *Lecture Notes in Control and Information Sciences*, 189-198, Springer-Verlag, Berlin.

Luo, Y., Chen, Y.Q., Wang, C.Y., and Pi, Y.G. (2010). Tuning fractional order proportional integral controllers for fractional order systems. *Journal of Process Control*, 20(7), 823–831.

Maâmar, B., and Rachid, M. (2014). IMC-PID-fractional-order-filter controllers design for integer order systems. *ISA Transactions*, 53(5), 1620–1628.

Malek, H., Luo, Y., and Chen, Y. (2013). Identification and tuning fractional order proportional integral controllers for time delayed systems with a fractional pole. *Mechatronics*, 23(7), 746–754.

Meneses, H., Arrieta, O., Padula, F., Vilanova, R., & Visioli, A. (2019). PI/PID control design based on a fractional-order model for the process. IFAC-PapersOnLine, 52(1), 976–981.

Monje, C.A., Chen, Y.Q., Vinagre, B.M., Xue, D., and Feliu, V. (2010). *Fractional-order Systems and Controls: Fundamentals and Applications*, Springer-Verlag, London.

Nagarsheth, S.H., and Sharma, S.N. (2020). The combined effect of fractional filter and Smith predictor for enhanced closed-loop performance of integer order time-delay systems: some investigations. Archives of Control Sciences, 30 (1), 47-76.

Pashaei, S., and Bagheri, P. (2019). Parallel cascade control of dead time processes via fractional order controllers based on Smith predictor. *ISA Transactions*, (in press).

Podlubny, I. (1999). Fractional-order systems and $PI^{\lambda}D^{\mu}$ controllers. *IEEE Transactions on Automatic Control*, 44 (1),208–14.

Tavakoli-Kakhki, M., & Haeri, M. (2011). Fractional order model reduction approach based on retention of the dominant dynamics: Application in IMC based tuning of FOPI and FOPID controllers. ISA Transactions, 50(3), 432–442.

Yumuk, E., Güzelkaya, M., and Eksin, İ. (2019). Analytical fractional PID controller design based on Bode's ideal transfer function plus time delay. *ISA Transactions*, 91, 196-206.